The Plant Cell, Vol. 11, 309–322, March 1999, www.plantcell.org © 1999 American Society of Plant Physiologists

RESEARCH ARTICLE

Cell-to-Cell and Long-Distance Trafficking of the Green Fluorescent Protein in the Phloem and Symplastic Unloading of the Protein into Sink Tissues

Astrid Imlau, Elisabeth Truernit, and Norbert Sauer[1]

Lehrstuhl Botanik II, Molekulare Pflanzenphysiologie, Universität Erlangen-Nürnberg, Staudtstrasse 5, D-91058 Erlangen, Germany

Macromolecular trafficking within the sieve element–companion cell complex, phloem unloading, and post-phloem transport were studied using the jellyfish green fluorescent protein (GFP). The *GFP* gene was expressed in Arabidopsis and tobacco under the control of the *AtSUC2* promoter. In wild-type Arabidopsis plants, this promoter regulates expression of the companion cell–specific *AtSUC2* sucrose–H^+ symporter gene. Analyses of the *AtSUC2* promoter–*GFP* plants demonstrated that the 27-kD GFP protein can traffic through plasmodesmata from companion cells into sieve elements and migrate within the phloem. With the stream of assimilates, the GFP is partitioned between different sinks, such as petals, root tips, anthers, funiculi, or young rosette leaves. Eventually, the GFP can be unloaded symplastically from the phloem into sink tissues, such as the seed coat, the anther connective tissue, cells of the root tip, and sink leaf mesophyll cells. In all of these tissues, the GFP can traffic cell to cell by symplastic post-phloem transport. The presented data show that plasmodesmata of the sieve element–companion cell complex, as well as plasmodesmata into and within the analyzed sinks, allow trafficking of the 27-kD nonphloem GFP protein. The data also show that the size exclusion limit of plasmodesmata can change during organ development. The results are also discussed in terms of the phloem mobility of assimilates and of small, low molecular weight companion cell proteins.

INTRODUCTION

Intercellular trafficking of macromolecules is involved in a variety of processes, including viral infection (reviewed in Maule, 1991; Lucas and Gilbertson, 1994; Carrington et al., 1996; Nelson and van Bel, 1998), tissue differentiation (Lucas et al., 1995), and the response to pathogen attack (Murillo et al., 1997). A further, well-studied example for cell-to-cell movement of macromolecules is the intercellular transport of phloem proteins (Bostwick et al., 1992; Fisher et al., 1992; Nakamura et al., 1993; Sakuth et al., 1993; Schobert et al., 1995; Balachandran et al., 1997; Kühn et al., 1997; Ishiwatari et al., 1998). In angiosperms, the phloem is composed mainly of two cell types, the sieve elements and their associated companion cells. Varying numbers of parenchymatic cells, fibers, and sclereids are also found in this tissue; however, it is thought that only the sieve element–companion cell complex is directly involved in long-distance translocation and partitioning of assimilates. Numerous mitochondria, plastids, and free ribosomes are responsible for an extraordinary density of the cytoplasm in companion cells, distinguishing them from all other cells of the phloem. In contrast, sieve elements are highly specialized for assimilate translocation, with most intracellular structures and organelles, such as nuclei, vacuoles, microtubules, ribosomes, and Golgi bodies, being degraded during sieve element development (Cronshaw, 1981; Behnke, 1989; Sjölund, 1997).

Sieve elements and companion cells are connected by numerous branched plasmodesmata, and, due to the often very long life span of sieve elements, which can range from weeks to months, it has frequently been suggested that these plasmodesmal connections are not only important for energy transfer and the flow of assimilates but also for the supply with macromolecular compounds, such as proteins (Raven, 1991). In analyses of soluble proteins of the sieve element sap of wheat (Fisher et al., 1992), rice (Nakamura et al., 1993; Ishiwatari et al., 1995), and *Ricinus communis* (Sakuth et al., 1993; Schobert et al., 1995), numerous proteins were identified that are assumed to be synthesized in the companion cells and to enter the sieve elements via the connecting plasmodesmata. Injection of fluorescent compounds into the stem phloem of broad bean (Kempers and van Bel, 1997) showed that the size exclusion limit (SEL) of the plasmodesmata connecting companion cells and sieve

[1]To whom correspondence should be addressed. E-mail nsauer@biologie.uni-erlangen.de; fax 49-9131-85-28751.

elements is somewhere between 10 and 40 kD, which is much higher than the SEL of plasmodesmata that connect nonphloem cells. This difference in the SEL of phloem and nonphloem plasmodesmata might be mediated by phloem proteins. Coinjection of phloem proteins with fluorescein isothiocyanate (FITC)–labeled dextrans into mesophyll cells of *Cucurbita maxima* caused an increase of the small basal SEL of the mesophyll cell plasmodesmata to values between 20 and 40 kD (Balachandran et al., 1997). Injection of FITC-labeled dextrans in the absence of phloem proteins showed no increase in SEL above the regular value of ~1 kD, which had previously been determined for mesophyll cells (Tucker, 1982; Goodwin, 1983; Wolf et al., 1989).

These results were interpreted to show the capability of phloem proteins to interact with plasmodesmata, to induce a significant increase in SEL, and to trigger their own trafficking through plasmodesmata (Balachandran et al., 1997). Recent studies with RPP13-1, a thioredoxin h protein from rice, confirmed these results, demonstrating that this protein can also mediate its own cell-to-cell transport through plasmodesmata (Ishiwatari et al., 1998).

In this study, we provide direct evidence that in Arabidopsis, a 27-kD nonphloem protein, the green fluorescent protein (GFP) from jellyfish (Chalfie et al., 1994), can migrate from cell to cell through plasmodesmata that link companion cells to sieve elements. In addition, we present data demonstrating that the GFP, after having entered the sieve elements, is freely mobile within the phloem and that it is translocated together with the stream of assimilates. Finally, using the GFP as a noninvasive tool, we demonstrate that this 27-kD protein is unloaded symplastically into numerous sink tissues, where it can traffick cell to cell by symplastic post-phloem transport.

RESULTS

AtSUC2 Promoter–*GFP* Plants Show *GFP* Expression Only in the Vascular System

Arabidopsis and tobacco plants expressing the GFP under the control of the companion cell–specific Arabidopsis *AtSUC2* promoter were generated and analyzed by excitation with short-wave blue light (450 to 490 nm). Two different promotor fragments and the entire 5′ untranslated sequence of the *AtSUC2* gene were used to generate two independent constructs (Figure 1). Regardless of the promoter length used (2160 or 945 bp), strong GFP fluorescence was detected specifically in the vascular system of the transgenic plants. Figure 2A shows a source leaf of an *AtSUC2* promoter–*GFP* plant photographed under blue light (460 to 490 nm), which causes red chlorophyll and yellowish GFP fluorescence. After overnight clearing, the same leaf was imaged in the dark field to visualize the complete veinal network (Figure 2B). Comparison of the fluorescent veins in Figure 2A and the veins in Figure 2B clearly shows that the *GFP* was expressed in every vein of the source leaf. This confirmed previous results in which *AtSUC2* promoter–driven β-glucuronidase (*GUS*) expression was shown to be confined to the phloem of Arabidopsis (Truernit and Sauer, 1995) and immunohistochemical analyses in which the AtSUC2 protein was found exclusively in the plasma membrane of companion cells (Stadler and Sauer, 1996). Thus, the GFP fluorescence seen in the Arabidopsis source leaf presented in Figure 2A is due to companion cell–specific expression of the *GFP* under the control of the *AtSUC2* promoter.

The GFP Can Pass Plasmodesmata from Companion Cells to Sieve Elements and Is Accumulated in Sink Leaves

An entire rosette of an *AtSUC2* promoter–*GFP* Arabidopsis plant is shown in Figure 3A. All source leaves show the yellowish green GFP fluorescence that is totally absent in the wild-type control presented in Figure 3C. However, an unexpected result was the strong GFP fluorescence detected in the small sink leaves in the center of the rosette and in the basal part of leaves that were in the transition status from sink to source (transition leaves). Identical results were obtained with tobacco plants expressing the *GFP* under the control of the *AtSUC2* promoter. Wild-type leaves showed only the red chlorophyll fluorescence (Figure 3D); however, in leaves of *AtSUC2* promoter–*GFP* tobacco plants, strong GFP fluorescence was again detected in the veins (Figure 3B). These results differ from earlier reports describing a source leaf–specific expression of *AtSUC2* (Truernit and Sauer, 1995). In these analyses, *AtSUC2* promoter–driven *GUS* expression started in the leaf tips during sink/source transition and was eventually found in the entire veinal network of fully developed source leaves (Truernit and Sauer,

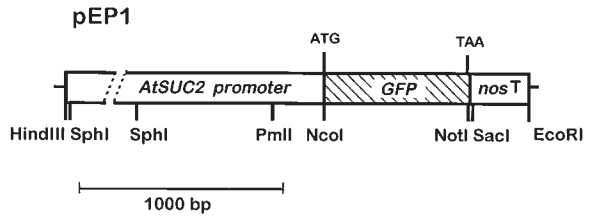

Figure 1. HindIII-EcoRI Insert of the pBI101-Derived Vector pEP1 That Was Used for Transformation of Arabidopsis and Tobacco Plants.

Removal of the 5′ 1215-bp SphI fragment yielded the vector pEPS1 with a truncated *AtSUC2* promoter. Both constructs gave identical *GFP* expression patterns in Arabidopsis and tobacco (*nos*T, terminator of the nopaline synthase gene).

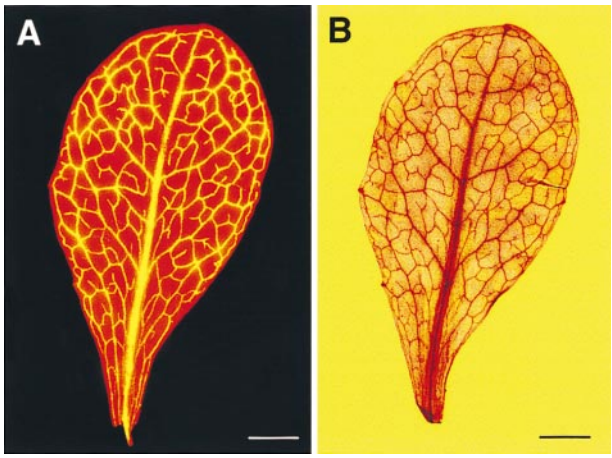

Figure 2. The *AtSUC2* Promoter Drives *GFP* Expression in the Phloem of All Vascular Bundles in Arabidopsis Source Leaves.

(A) Red chlorophyll and strong, yellowish GFP fluorescence in a source leaf of an Arabidopsis *AtSUC2* promoter–*GFP* plant after excitation with light of 450 to 490 nm.
(B) Same leaf as shown in **(A)** but cleared overnight in ethanol–acetic acid (7:1) and imaged in dark field. All veins show similar levels of GFP expression.
Bars = 2 mm.

1995; Figures 3E and 3F). *GUS* expression was never seen in sink leaves or in the sink areas of transition leaves.

We suspected that these differing results obtained with *AtSUC2* promoter–*GUS* plants and *AtSUC2* promoter–*GFP* plants were due to differences in the phloem mobility of the two reporter gene products. Unlike the previously used *AtSUC2* promoter–*GUS* construct (Truernit and Sauer, 1995) that comprised a translational fusion of GUS to 53 N-terminal amino acids of the AtSUC2 protein, including the first transmembrane helix and yielding a membrane-bound protein, the *AtSUC2* promoter–*GFP* construct used in this work is not a translational fusion. The recombinant GFP starts with its own methionine (Figure 1) and is a soluble 27-kD protein. This molecular mass of the GFP is within the size range described for the SEL of the plasmodesmata connecting companion cells and sieve elements with values between 20 and 40 kD (Balachandran et al., 1997; Kempers and van Bel, 1997) and thus may allow the passage of the GFP from companion cells into sieve elements. Once inside the sieve elements, the GFP should be passively translocated, and the direction of its movement should be determined by the pathway of the photoassimilates. Such a passive flow inside the sieve elements has previously been reported for viral particles (Leisner et al., 1992; Roberts et al., 1997) and for synthetic compounds (Oparka et al., 1994).

This hypothesis is supported by a more detailed anaylsis of GFP fluorescence in sink and transition leaves (Figure 4). The vein classification used for this analysis is based on the vein classifications for *Nicotiana tabacum* and *N. benthamiana* (Avery, 1933; Ding et al., 1988; Roberts et al., 1997). During leaf development, GFP fluorescence is first seen in the midrib (class I vein) of the smallest sink leaves (Figure 4B). In more developed sink leaves (smaller leaf in Figure 4A), GFP fluorescence is also detected in class II veins that branch from the midrib and eventually interconnect at the leaf margins (top of the leaf). In transition leaves (larger leaf in Figure 4A), GFP fluorescence is seen in all veins of the leaf tip (source region) but almost exclusively in class I and class II veins at the leaf basis (sink region). Hardly any or no GFP

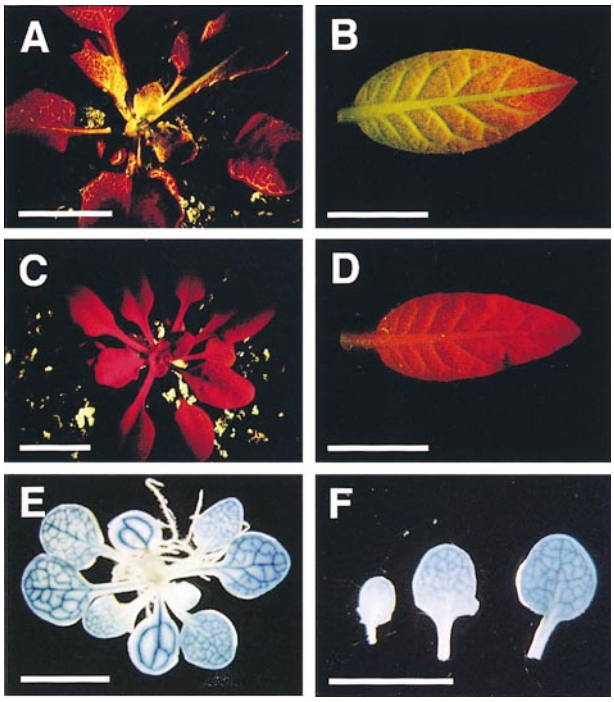

Figure 3. Comparison of *AtSUC2* Promoter–*GFP* Plants and *AtSUC2* Promoter–*GUS* Plants.

(A) Rosette of an Arabidopsis plant expressing *GFP* under the control of the *AtSUC2* promoter. *GFP* expression is seen in all veins of the source leaves. The stronger GFP fluorescence in sink and transition leaves is due to influx of the GFP synthesized in the source leaves.
(B) Transition leaf from a tobacco plant expressing the GFP under the control of the *AtSUC2* promoter.
(C) Rosette of an Arabidopsis wild-type plant showing only red chlorophyll fluorescence.
(D) Leaf from a tobacco wild-type plant showing only red chlorophyll fluorescence.
(E) and **(F)** GUS histochemical staining of an *AtSUC2* promoter–*GUS* rosette **(E)** and three leaves of this rosette **(F)** showing no *AtSUC2* promoter activity in the sink regions and progressive GUS staining during the sink/source transition.
Bars in **(A)** to **(F)** = 1 cm.

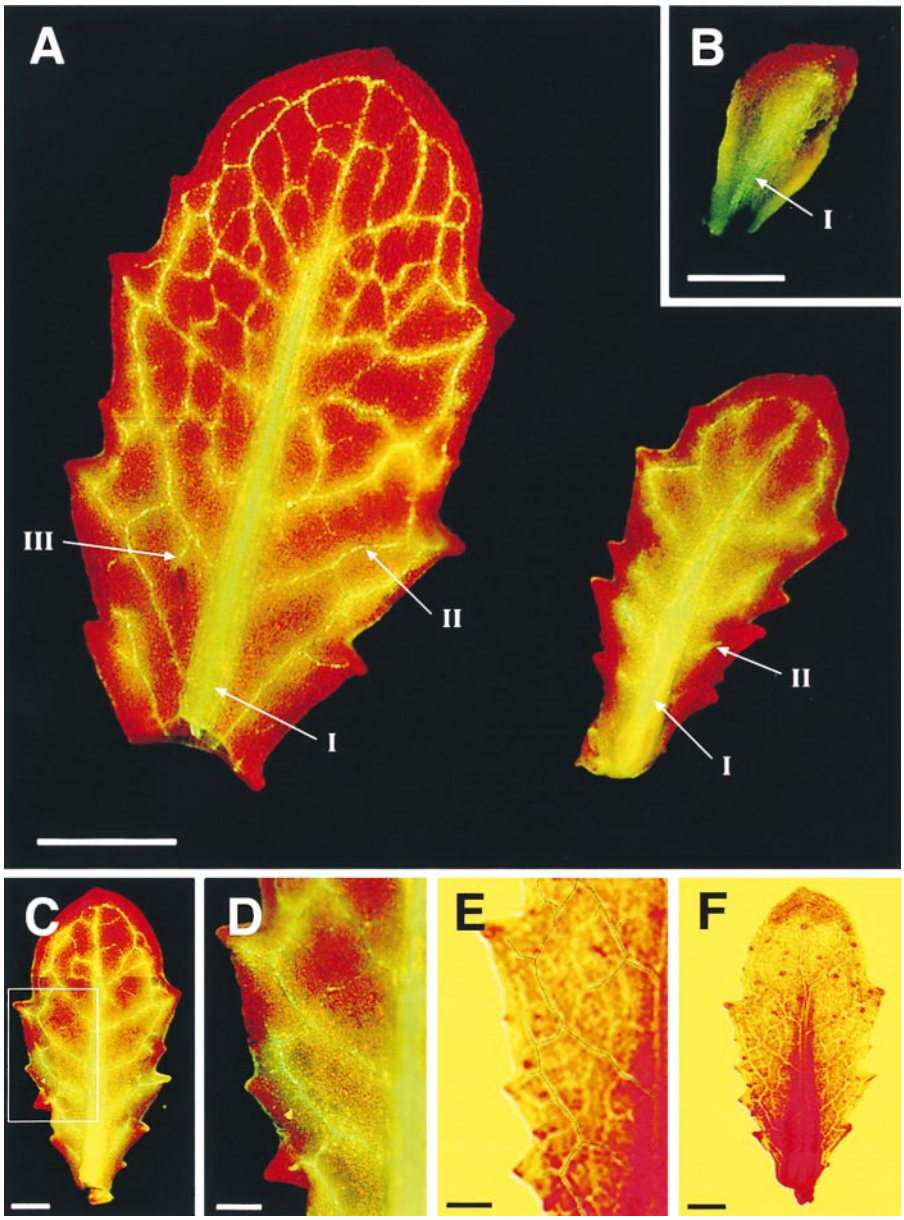

Figure 4. GFP Fluorescence in Sink Leaves from *AtSUC2* Promoter–*GFP* Arabidopsis Plants at Different Developmental Stages.

(A) Red chlorophyll and yellowish green GFP fluorescence in a sink leaf (smaller leaf) and a leaf during the sink/source transition (larger leaf) after excitation with light of 450 to 490 nm. Diffusion of the GFP from the phloem can be detected in the smaller sink leaf and in the basal sink region of the transition leaf. In both leaves, the veinal network is more developed in the leaf tip than in the leaf base. Typical veins of classes I, II, and III are marked with arrows. Bar = 500 μm.
(B) Fluorescence of a very young sink leaf taken from the same plant as the leaves shown in **(A)**. GFP fluorescence can only be detected in the midrib (class I vein) and in the adjacent mesophyll cells. Bar = 200 μm.
(C) Young leaf with beginning sink/source transition and strong symplastic unloading of the GFP from class I and class II veins. Bar = 500 μm.
(D) Enlargement of the boxed region in **(C)**. Bar = 250 μm.
(E) Same leaf as shown in **(D)** cleared overnight in ethanol–acetic acid (7:1). The faint dark lines depict the GFP fluorescence in **(D)**. Numerous minor veins can be detected that show no GFP fluorescence in **(D)**. Bar = 250 μm.
(F) Same leaf as shown in **(C)** that was cleared overnight in ethanol–acetic acid (7:1). Numerous minor veins can be detected that show no GFP fluorescence in **(C)**. Bar = 500 μm.

fluorescence can be detected in class III veins of the sink regions of these transition leaves, although class III and even class IV veins are already present and can be made visible after clearing the leaves in ethanol–acetic acid (Figures 4C to 4F). This distribution pattern of the GFP in the sink leaf veinal network compares well with the reported influx of carboxyfluorescein into tobacco sink leaves after the application of this fluorescent dye to expanded source leaves (Roberts et al., 1997). Carboxyfluorescein moves with the stream of assimilates and was shown to enter classes I, II, and III veins of tobacco sink leaves. Minor veins (classes IV and V veins in tobacco) were not accessible to carboxyfluorescein (Roberts et al., 1997).

The GFP Can Be Symplastically Unloaded from Classes I, II, and III Veins but Not from Minor Veins

An interesting observation was the obvious unloading of the GFP from the fluorescing veins in sink leaves and from the fluorescing veins in the sink regions of transition leaves. This unloading caused a gradient of GFP fluorescence into the adjacent mesophyll cells and occurred from class I and class II veins and to some extent also from class III veins of sink leaves. Because the GFP does not enter the minor veins of these leaves (Figures 4E and 4F), these veins were not involved in the symplastic unloading of the GFP to the mesophyll. After the onset of the sink/source transition, unloading of the GFP ceased and was no longer detected in the source regions of transition leaves (note the lack of green haze around veins in the upper third of the larger leaf in Figure 4A) or in fully developed source leaves (Figure 2), which may indicate a reduction in the SEL of the plasmodesmata of these cells.

The GFP Can Migrate from Transgenic Tobacco Rootstocks into Wild-Type Scions

For independent proof of the phloem mobility of the GFP, we grafted wild-type tobacco plants onto tobacco plants transformed with pEP1 (Figure 1) and analyzed the scions for their GFP content. If the GFP produced in the companion cells of the transgenic rootstock enters the sieve elements, then it should be translocated into the grafted wild-type scion. Figure 5A shows a cross-section through the petiole of a wild-type tobacco leaf with faint yellowish fluorescence of the xylem vessels. A similar section through the petiole of transition leaf of an *AtSUC2* promoter–*GFP* tobacco plant shows strong additional GFP fluorescence in both parts of the bicollateral phloem (Figure 5B). GFP fluorescence can also be seen in sections through petioles of sink or transition leaves from wild-type scions that had been grafted onto *AtSUC2* promoter–*GFP* tobacco plants (Figure 5C). The fluorescence in grafted wild-type leaves is sometimes

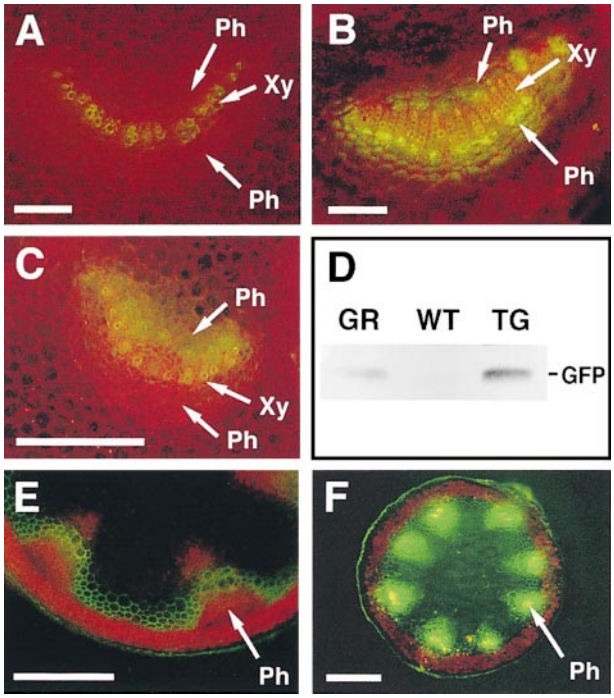

Figure 5. Identification of GFP Fluorescence and the GFP in Sink Leaves of Wild-Type Tobacco Plants after Grafting on *GFP*-Expressing Tobacco Rootstocks.

(A) Section through the petiole of a wild-type tobacco plant imaged under blue excitation light. The faint yellow fluorescence is due to the phenolics deposited in the xylem vessels. No fluorescence is seen in any part of the bicollateral phloem.

(B) Section through the petiole of an *AtSUC2* promoter–*GFP* tobacco plant imaged under blue excitation light. In addition to the yellowish fluorescence in the xylem, strong green GFP fluorescence is seen in both regions of the phloem.

(C) Section through the petiole of a wild-type tobacco plant that had been grafted onto a plant expressing *GFP* under the control of the *AtSUC2* promoter. Photography was under blue excitation light. In addition to the yellowish fluorescence in the xylem, green GFP fluorescence is seen in the upper half of the bicollateral phloem.

(D) Protein gel blot analyses of SDS-solubulized protein extracts from sink leaves of wild type (WT), transgenic (TG), and grafted wild-type (GR) tobacco plants. Identical amounts of protein were loaded per lane, and the GFP was identified by using a polyclonal anti-GFP antiserum.

(E) Section through the inflorescence stem of a wild-type Arabidopsis plant imaged under blue excitation light. The green fluorescence is due to the phenolics deposited in the xylem vessels. No fluorescence is seen in any part of the phloem.

(F) Section through the inflorescence stem of an *AtSUC2* promoter–*GFP* Arabidopsis plant imaged under blue excitation light. The strong green fluorescence in the phloem (which turns to yellow at the point of highest intensity) is due to *GFP* expressed in the phloem. The green fluorescence in the epidermis is not due to GFP expression and is also seen in the control section shown in **(E)**.

Ph, phloem; Xy, xylem. Bars in **(A)** to **(C)**, **(E)**, and **(F)** = 200 μm.

weaker than the fluorescence in comparable leaves of the *AtSUC2* promoter–*GFP* tobacco plant, which may be due to the varying number of phloem vessels forming continuous connections during the grafting process. Nevertheless, the fluorescence in the scion is clearly due to the imported GFP protein, which can be detected on protein gel blots of extracts from grafted wild-type plants (Figure 5D). No band is seen in extracts from sink leaves of wild-type tobacco plants that had not been grafted. These results prove that the GFP produced in companion cells of the transgenic rootstock is indeed translocated over long distances within the sieve elements.

Interestingly, GFP fluorescence in the phloem of grafted tobacco wild-type plants (Figure 5C) is always confined to the upper half of the bicollateral phloem, which is connected to the adaxial phloem of the stem. This suggests that assimilate influx into sink and transition leaves of tobacco occurs only from the adaxial and not from the abaxial phloem.

The GFP Is Symplastically Unloaded into Floral Organs

Floral organs, such as petals, anthers, and developing ovules, but also the growing embryo, are strong sinks and need to be supplied with large amounts of assimilates. The strong GFP fluorescence that was detected in the inflorescence stems of *AtSUC2* promoter–*GFP* Arabidopsis plants may reflect this assimilate flux (Figures 5E and 5F). The mechanism of phloem unloading (symplastic or apoplastic) into the various sinks of an Arabidopsis flower is largely unknown.

It has previously been shown that the *AtSUC2* promoter is not or is barely active in the phloem of petals of *AtSUC2* promoter–*GUS* plants (Truernit and Sauer, 1995). The white, photosynthetically inactive petals represent a permanent sink tissue that is highly dependent on assimilate influx from the phloem. Figure 6A shows a flower of an *AtSUC2* promoter–*GUS* plant stained with 2-(2,4-hydroxy-3-methoxyphenyl)vinyl-1-methylquinolinium iodine, a substrate for the GUS protein yielding a red color. Clearly, there is strong staining in the phloem of the sepals and stamens, but there is no detectable GUS activity in the petals. In contrast, Figures 6B to 6D show strong GFP fluorescence in the phloem of petals from *AtSUC2* promoter–*GFP* plants. Moreover, the GFP diffuses into the adjacent cells of the petal mesophyll, causing a gradient of fluorescence similar to that seen in developing sink leaves of the rosette (Figure 4). These results show that the GFP synthesized in the source tissues is transported together with the assimilates into the phloem of the petals, and that the GFP, and thus also the assimilates, can be symplastically unloaded. No fluorescence is seen in a wild-type control flower (Figures 6E and 6F). The fluorescence seen in the wild-type anther (Figure 6E) is due to deposition of phenolics in the pollen exine and in the outermost cell layers of the anther wall during the late stages of anther development. It is not seen in developmentally younger anthers before anther dehiscence (Figure 6H).

Import of assimilates is also important for anthers in which assimilates are needed for the growth and development of the male gametophyte. In Figure 6G, the phloem catalyzing this assimilate influx into an Arabidopsis anther is visualized by the blue GUS staining in the stamen of an *AtSUC2* promoter–*GUS* plant showing the phloem ending in the connective tissue. Analysis of GFP fluorescence in anthers of *AtSUC2* promoter–*GFP* plants revealed GFP fluorescence not only in the phloem: strong fluorescence was also detected in the adjacent cells of the connective tissue (Figure 6I), and a gradient of GFP fluorescence spreads from the connective tissue toward the anther locules. This indicates symplastic unloading of the GFP in *AtSUC2* promoter–*GFP* plants from the phloem ends into the anther connective tissue and suggests that assimilates are also symplastically unloaded from the phloem into this tissue. No green fluorescence was detected in the anthers of wild-type Arabidopsis plants at the same developmental stage (Figure 6H).

Assimilated carbon is also supplied to the developing embryo. The vascular bundle is connected to the ovule by the funiculus that ends at the nucellar tissue of the ovule. No vascular tissue extends beyond the funiculus into the ovule (Bowman, 1994). In previous studies with *AtSUC2* promoter–*GUS* plants, GUS histochemical staining was confined to the vascular tissue of the funiculus, and no GUS activity was detected in ovules (Truernit and Sauer, 1995; Figure 7E). In immunohistochemical studies with the anti-AtSUC2 antiserum, the AtSUC2 protein was detected only in the companion cells of the funicular phloem but not in any other part of the ovules (R. Stadler and N. Sauer, unpublished data). In ovules from *AtSUC2* promoter–*GFP* plants, strong GFP fluorescence can be seen in the nucellar region, and this fluorescence is spreading into the cell layers of the seed coat (Figures 7A and 7C). Only minimal GFP fluorescence can be seen in the center of the ovule, where the embryo is located. More detailed analyses of this GFP fluorescence in Arabidopsis ovules, using a confocal laser scanning microscope, confirmed these results, showing GFP fluorescence only in the seed coat of the transgenic ovules (Figure 7F). No green fluorescence was observed in embryos developing on GFP-expressing plants (Figure 7H) or in ovules from wild-type plants that were analyzed under identical conditions (Figures 7B, 7D, and 7G).

This localization of the GFP in ovules of *AtSUC2* promoter–*GFP* plants suggests that the GFP is symplastically unloaded from the funicular phloem into the nucellus. From there, the GFP can migrate symplastically cell to cell into and within the seed coat. Moreover, these results indicate that the plasmodesmata connecting the phloem cells of the funiculus with the nucellar cells and also the plasmodesmata of the cells of the seed coat have plasmodesmata with a similar SEL to that of the plasmodesmata connecting sieve elements and companion cells.

Figure 6. Accumulation and Symplastic Unloading of the GFP in Petals and Anthers of *AtSUC2* Promoter–*GFP* Arabidopsis Plants.

(A) Histochemical analysis of a flower of an *AtSUC2* promoter–*GUS* plant stained with 2-(2,4-hydroxy-3-methoxyphenyl)vinyl-1-methylquinolinium iodine. GUS activity is confined to the phloem of the sepals and the stamens. No GUS activity is detectable in the petals. Bar = 1 mm.
(B) Flower of an *AtSUC2* promoter–*GFP* plant photographed under blue excitation light. Bar = 1 mm.
(C) Same flower as shown in **(B)** photographed in white light. Bar = 1 mm.
(D) Strong GFP fluorescence in petals and comparatively low GFP fluorescence in sepals of an *AtSUC2* promoter–*GFP* plant. Bar = 1 mm.
(E) Flower of an Arabidopsis wild-type plant photographed under blue excitation light. Bar = 1 mm.
(F) Same flower as shown in **(E)** photographed in white light. Bar = 1 mm.
(G) Anther of an *AtSUC2* promoter–*GUS* Arabidopsis plant. The blue GUS histochemical staining depicts the position of the phloem (p) in this stamen. Bar = 100 μm.
(H) Anther of an Arabidopsis wild-type plant photographed under blue excitation light. No yellow or green fluorescence is detectable. Bar = 100 μm.
(I) Anther of an *AtSUC2* promoter–*GFP* plant photographed under blue excitation light. The GFP is confined to the phloem of the filament, is symplastically unloaded into the anther connective tissue, and diffuses toward the anther locules. Bar = 100 μm.

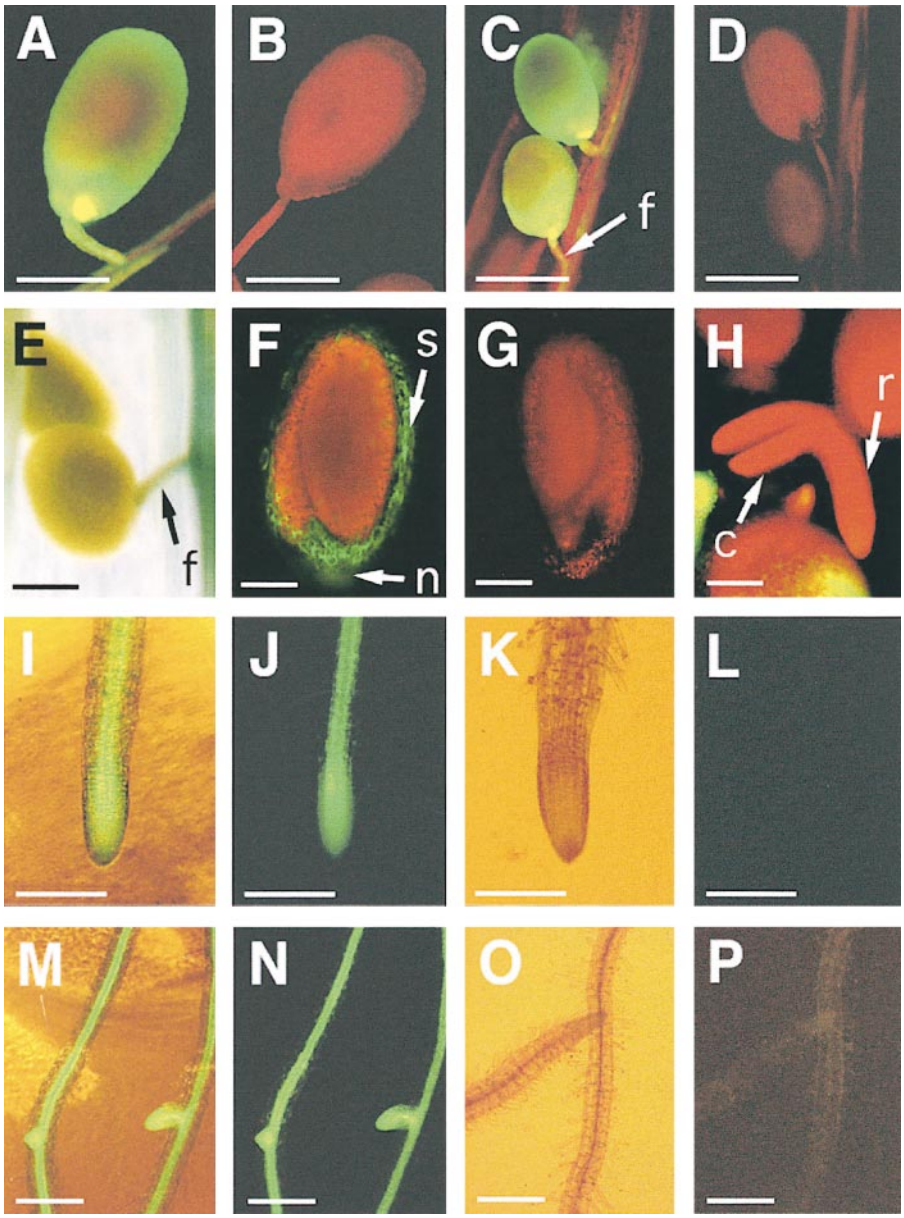

Figure 7. Symplastic Unloading of the GFP into Ovules and Root Tips of *AtSUC2* Promoter–*GFP* Arabidopsis Plants.

(A) Green GFP fluorescence (that turns yellow at the point of highest GFP concentration) and red chlorophyll fluorescence in an ovule of an *AtSUC2* promoter–*GFP* plant. GFP fluorescence is stronger at the surface of the ovule, resulting in a red center that is due to chlorophyll fluorescence from the developing embryo. Bar = 250 μm.

(B) Red chlorophyll fluorescence in an ovule of an Arabidopsis wild-type plant. Bar = 250 μm.

(C) Ovules in the silique of an *AtSUC2* promoter–*GFP* Arabidopsis plant at lower magnification. The GFP fluorescence is stronger at the surface of the ovules, resulting in red centers that are due to chlorophyll fluorescence from the developing embryos. f, funiculus. Bar = 500 μm.

(D) Ovules in the silique of Arabidopsis wild-type plant at lower magnification. No GFP fluorescence is seen in these ovules. Bar = 500 μm.

(E) Histochemical staining of a silique from an *AtSUC2* promoter–*GUS* Arabidopsis plant. Blue GUS staining is only detectable in the longitudinal phloem and in the funiculus (f). No GUS staining is detectable in the seed coat. Bar = 250 μm.

(F) Red chlorophyll and green GFP fluorescence in an optical section through an ovule of an *AtSUC2* promoter–*GFP* Arabidopsis plant in 488-nm excitation light. GFP fluorescence is confined to the seed coat (s) and the nucellar region (n). No GFP fluorescence is seen in the embryo. Bar = 125 μm.

(G) Red chlorophyll fluorescence in an optical section through an ovule of an Arabidopsis wild-type plant in 488-nm excitation light. Bar = 125 μm.

The GFP Is Symplastically Unloaded at the Root Tip

In *AtSUC2* promoter–*GUS* plants, GUS activity was detected in the root phloem (Truernit and Sauer, 1995), and the AtSUC2 protein was also identified in companion cells of Arabidopsis root phloem by using the anti-AtSUC2 antiserum (Stadler and Sauer, 1996). No AtSUC2 protein and no GUS activity were detected in the very tips of Arabidopsis roots when these techniques were used. Oparka et al. (1994) reported that carboxyfluorescein that had been supplied through the leaves was symplastically unloaded from the phloem in the root tips of Arabidopsis. Analyses of GFP fluorescence in the roots of *AtSUC2* promoter–*GFP* plants confirmed these results. GFP fluorescence was confined to the phloem all along the roots but seemed to bleed from the phloem ends at the root tips (Figures 7I and 7J) and at the sites of lateral root formation (Figures 7M and 7N). This was caused by the symplastic unloading of the GFP into the cells of the root tips and resulted in a diffuse fluorescence at the zone of cell division. No fluorescence was seen in the roots of wild-type control plants (Figures 7K, 7L, 7O, and 7P). This result shows that plasmodesmata that allow the trafficking of the GFP out of the phloem in the root tips decrease their SEL during their further development, because no GFP trafficking is seen in the zones above the root tip.

DISCUSSION

The GFP Can Traffic Cell to Cell from Companion Cells into Sieve Elements

The GFP of jellyfish moves cell to cell through plasmodesmata from companion cells into sieve elements in Arabidopsis and tobacco plants expressing the *GFP* gene under the control of the companion cell–specific *AtSUC2* promoter. This indicates that cell-to-cell trafficking through plasmodesmata with an SEL between 10 and 40 kD (Balachandran et al., 1997; Kempers and van Bel., 1997) is not confined to phloem proteins in source leaves or to viral movement proteins (Fujiwara et al., 1993). Plasmodesmal localization domains have frequently been discussed as a prerequisite for cell-to-cell trafficking of soluble proteins. Examples are phloem proteins, such as thioredoxin h (Ishiwatari et al., 1998), which can mediate its own cell-to-cell transport, and phloem protein 2 (PP2), cystatin, and glutaredoxin, which can increase the plasmodesmal SEL to values between 20 and 40 kD (Balachandran et al., 1997). Mutational analyses of the 35-kD movement protein of red clover mosaic virus also suggested that for this protein, there is a distinct functional domain responsible for plasmodesmal trafficking (Fujiwara et al., 1993). The jellyfish GFP is unlikely to possess specific sequences for interaction with plasmodesmal structures, although an interaction cannot be fully excluded.

Export Rather Than Retention May Be the Default Pathway for Soluble Proteins of the Companion Cells

The crystal structure of the GFP has previously been determined, and it has been shown to have a barrel-like shape forming a nearly perfect cylinder 42 Å long and 24 Å in diameter (Ormö et al., 1996). The GFP is exceptionally resistant to chemical and physical treatments, such as heat, alkaline pH, detergents, or organic solvents (Bokman and Ward, 1981; Ward, 1981). Therefore, unfolding and refolding of the GFP during the trafficking step seems unlikely, although chaperones have been identified in the sieve-tube exudate of *R. communis* (Schobert et al., 1995), and a potential role of these chaperones in the plasmodesmal trafficking of large proteins has been discussed (Schobert et al., 1995; Balachandran et al., 1997).

Figure 7. (continued).

(H) Red chlorophyll fluorescence in a developing embryo that has been isolated from its surrounding seed coat. The ovule was taken from the silique of an *AtSUC2* promoter–*GFP* plant. Cotelydons (c) and radicle (r) are entirely devoid of any GFP fluorescence. Bar = 125 μm.
(I) GFP fluorescence in the root tip of an *AtSUC2* promoter–*GFP* plant. Photography was under blue excitation light and low-intensity white light simultaneously. Unloading of the GFP from the phloem into the root tip results in a diffuse GFP fluorescence that is no longer confined to the phloem. Bar = 300 μm.
(J) Same root tip as shown in **(I)** but imaged under blue excitation light only. Bar = 300 μm.
(K) Root tip of an Arabidopsis wild-type plant. Photography was under blue excitation light and low-intensity white light simultaneously. No GFP fluorescence is seen in this root tip. Bar = 300 μm.
(L) Same root tip as shown in **(K)** but imaged under blue excitation light only. Bar = 300 μm.
(M) Roots of an *AtSUC2* promoter–*GFP* Arabidopsis plant with emerging lateral roots at a lower magnification. Photography was under blue excitation light and low-intensity white light simultaneously. As shown in **(I)**, unloading of the GFP from the phloem into the tips of the lateral roots results in a diffuse GFP fluorescence that is not confined to the phloem. Bar = 300 μm.
(N) Same roots as shown in **(M)** but imaged under blue excitation light only. Bar = 300 μm.
(O) Roots of an Arabidopsis wild-type plant imaged under blue excitation light and low-intensity white light simultaneously. No GFP fluorescence is detectable in these roots. Bar = 300 μm.
(P) Same roots as shown in **(I)** but imaged under blue excitation light only. Bar = 300 μm.

Support for this model comes from the observation that FITC-labeled dextrans of 10 or 20 kD can traffic through plasmodesmata opened by phloem proteins (Balachandran et al., 1997; Kempers and van Bel, 1997), which suggests that molecules with the proper molecular weight may migrate simply by passive diffusion. However, it was shown by Balachandran et al. (1997) that an FITC-labeled C-terminal deletion mutant of ubiquitin with a molecular mass of only ~8 kD was not able to traffic through plasmodesmata opened by the phloem protein PP2. This indicates that the molecular mass may not be the only criterion for trafficking through plasmodesmata. It has been postulated that ubiquitin may require the presence of a companion cell–specific protein(s) to mediate its transport into the sieve element system (Balachandran et al., 1997). However, this model does not explain why, in the absence of this postulated helper protein, the 8-kD ubiquitin would stay inside the companion cells, whereas a 20-kD dextran can migrate into the adjacent sieve elements. This can only be explained by a retention mechanism preventing the undesirable loss of low molecular weight proteins from the companion cells.

If such a retention mechanism exists, apparently it does not prevent the cell-to-cell trafficking of the GFP into sieve elements. We therefore suggest that the GFP does not interact with plasmodesmal structures and that it moves by passive diffusion from the companion cells into the sieve elements. This may also apply to other soluble companion cell proteins that do not possess specific retention signals, suggesting that export from the companion cells rather than retention may be the default pathway of these proteins.

The GFP Is Translocated within the Sieve Elements and Can Be Unloaded Symplastically

It is well known that during the early stages of leaf development, assimilated carbon is imported from fully developed source leaves (reviewed in Turgeon, 1989). This carbon import has been studied in detail by feeding radiolabeled CO_2 to source leaves of *C. pepo* (Turgeon and Webb, 1973), beet (Turgeon and Webb, 1973; Fellows and Geiger, 1974), and tomato (Ho and Shaw, 1977). Analyses of the incorporation of radiolabeled assimilates into developing sink leaves revealed that in all of these plants, the sink/source transition started in the leaf tip and proceeded toward the leaf base. The activity of the companion cell–specific *AtSUC2* promoter (Stadler and Sauer, 1996) was shown to correlate with this sink/source transition in Arabidopsis (Truernit and Sauer, 1995).

After its synthesis in *AtSUC2* promoter–*GFP* plants and after its passage from companion cells into sieve elements, the GFP is obviously translocated with the stream of assimilates toward the various sinks. This is confirmed by the identification of GFP fluorescence in sections of sink leaves from grafted wild-type plants (Figure 5C) and of the GFP in leaf extracts of wild-type tobacco plants that had been grafted onto GFP-expressing transgenic tobacco (Figure 5D).

The phloem mobility of the GFP within the sieve elements of Arabidopsis is also demonstrated in Figures 6 and 7, which show strong GFP fluorescence in the phloem of several Arabidopsis tissues in which the *AtSUC2* promoter was not or was barely active. This presence of the GFP in sink tissues, such as petals, anthers, root tips, and seeds, can only be explained by the influx of the GFP. Moreover, the detailed comparison of GUS histochemical staining and GFP fluorescence in these sink organs reveals the mechanisms of phloem unloading. The GFP fluorescence seen in the ovules shown in Figures 7A and 7C can only result from symplastic unloading of the GFP into the nucellar tissue and from symplastic post-phloem cell-to-cell trafficking of the GFP within the cells of the seed coat. This result is supported by data from Wang and Fisher (1994a, 1994b), who determined increased SELs for plasmodesmata from tissues involved in post-phloem transport of assimilates in wheat grains.

Figures 4, 6, and 7 demonstrate that GFP fluorescence spreads from the ends of the phloem into adjacent cells in all sink tissues analyzed (anthers, root tips, petals, and sink leaves of the rosette). This indicates that phloem unloading and post-phloem transport of assimilates are symplastic and that the plasmodesmata of the cells involved in post-phloem transport also have an SEL of at least 27 kD.

Symplastic phloem unloading has been described previously for root tips of Arabidopsis. Oparka et al. (1994) showed that the synthetic fluorescent compound 5(6)-carboxyfluorescein flows with the stream of assimilates into Arabidopsis roots and that this synthetic compound is symplastically unloaded from the phloem into the root tip.

Developing Gametophytes Are Symplastically Isolated

No GFP fluorescence was detected in embryos developing on GFP-expressing plants (Figures 7F and 7H), suggesting that no or only a few symplastic connections exist between the embryo and the surrounding seed coat. This coincides with the description of an exclusively apoplastic import of sugars into the developing embryo of broad bean (Weber et al., 1997). In this work, a monosaccharide transporter (VfSTP1) and a disaccharide transporter (VfSUT1) were identified in epidermal cells of embryos of broad bean (*Vicia faba*). These cells showed transfer cell morphology and are responsible for the uptake of carbohydrates from the apoplastic space.

A similar situation exists in anthers in which symplastic post-phloem transport of the GFP is seen (Figure 6I). This post-phloem transport can proceed toward the cells of the middle layer, which show no further symplastic connections to the tapetal cells (Clément and Audran, 1995). The middle layer cells are assumed to act as a physiological buffer regulating the amount of sugars delivered to the locular fluid (Pacini and Franchi, 1983; Clément and Audran, 1995). A plasma membrane–localized transporter in developing pollen has only recently been described (Truernit et al., 1999).

The SEL of Plasodesmata Is Regulated during Cell Development

The large SEL of the plasmodesmata connecting the phloem ends with the cells of different sink tissues is not constant during development. Symplastic unloading of the GFP into root tips and in sink leaves (Figures 4A, 4B, and 7I to 7P) ceases during root and leaf development. The GFP is not unloaded from the developmentally older phloem in the zones above the root tip (Figures 7I to 7P) or from the phloem in source leaves (Figures 2 and 4B). In the latter case, this may be explained by a reversal in the direction of the assimilate flow, which is directed into the sink leaves and out of the source leaves. Symplastic unloading of the GFP from the veins of source leaves therefore may not be possible. However, only a few plasmodesmata were found between the sieve element–companion cell complex of Arabidopsis and their adjacent cells (Gamalei, 1989), and companion cells in tobacco minor veins were shown to be symplastically isolated from their adjacent parenchyma and bundle sheath cells (Ding et al., 1995). This suggests that the lack of symplastic unloading from veins of source leaves is due to a drastically reduced number of plasmodesmata (Ding et al., 1988) or to a reduction in the SEL.

The situation is clearer in roots, where the direction of the assimilate flow stays constant during development. Again, the lack of symplastic GFP unloading in the more developed areas of the root (above the root tip) can only be explained by either a reduction of the SEL or a decrease in the number of functionally active plasmodesmata.

Other Macromolecules and Virus Particles May Follow the Path of the GFP

Our results reveal that sink leaf mesophyll cells, cells of the seed coat, and cells of the root tip or the connective tissue form a functional extension of the phloem. An advantage of this symplastic continuity beyond the ends of the phloem may be the drastic increase in cell surfaces that are involved in the release of assimilates into the apoplast for further carrier-mediated and thus well-controlled transport steps.

However, the identification of macromolecular trafficking of the GFP from source leaves into various sink tissues not only allows us to predict the direction of the assimilate flow but, most importantly, also allows us to predict the pathway of signaling molecules and virus particles that will passively follow the stream of assimilates. An example is the recent report on the symplastic unloading of GFP-labeled potato virus X in class III veins of tobacco sink leaves (Roberts et al., 1997). Viral particles applied to a source leaf migrated within the phloem but were unable to enter the minor veins in the sink leaf. This result agrees perfectly with the distribution of the phloem-mobile GFP in Arabidopsis sink leaves (Figure 4).

What Happens to Soluble Sieve Element Proteins in the Sinks?

The fate of the GFP that is synthesized in companion cells and that accumulates in or at sink tissues raises a general question about the fate of a plant's own soluble phloem proteins. The accumulation of the GFP in sink tissues suggests that several (or all) of the previously identified soluble sieve element proteins may also flow toward these tissues together with the assimilates. Eventually, these proteins may be metabolized and thus serve as a source of amino acids or peptides. It is necessary to measure both the precise concentration of sieve element proteins in the phloem sap and their translocation rate to determine their potential role in the carbon and nitrogen supply of sink tissues.

METHODS

Strains

Escherichia coli DH5α (Hanahan, 1983) was used for cloning. For transformation of *Arabidopsis thaliana* C24 and *Nicotiana tabacum* cv Sumsai, *Agrobacterium tumefaciens* LBA4404 (Ooms et al., 1982) was used. Arabidopsis and tobacco plants were grown in potting soil in the greenhouse or on agar medium in plastic containers, as previously described (Truernit and Sauer, 1995).

Generation of *AtSUC2* Promoter–*GFP* Plants and Determination of GFP Activity

A polymerase chain reaction (PCR) was performed with the oligonucleotides HP-SUC2P (5′-CCGGAAGCTTCACGTGTCACGAAGATACCC-3′; HindIII and PmlI sites underlined) and SNN-SUC2P (5′-CCGGGAGCTCGCGGCCGCTGCCCCATGGTTGACAAACCAAGAAAGTAA-3′; SacI, NotI, and NcoI sites underlined) and the plasmid pET212 (Truernit and Sauer, 1995). The pUC19-based plasmid pET212 harbors the *AtSUC2* promotor, the β-glucuronidase *GUS* reporter gene, and the nopaline synthase terminator. The resulting PCR fragment started at a unique PmlI site 228 bp upstream from the *AtSUC2* start ATG and introduced a unique NcoI cloning site at this start ATG (by changing the 5′ flanking AT to CC) followed by additional cloning sites for NotI and SacI. The identity of this fragment was confirmed by sequencing (Sanger et al., 1977). The PmlI-SacI–digested PCR fragment was inserted into the respective sites of pET212 to remove the *GUS* reporter gene. The resulting plasmid contained the *AtSUC2* promotor and the nopaline synthase terminator separated by unique NcoI and NotI cloning sites. These sites were used to insert 730 bp of the green fluorescent protein (*GFP*) coding sequence isolated as an NcoI-NotI fragment from the plasmid pGFP-TYGpA-K (Chiu et al., 1996), yielding plasmid pEP/pUC19. A 2900-bp HindIII-SacI fragment containing 2159 bp of *AtSUC2* promotor followed by the *GFP* coding sequence was excised from pEP/pUC19 and cloned into pBI101 (Jefferson et al., 1987), yielding plasmid pEP1. Excision of a 1214-bp SphI fragment from pEP1 yielded plasmid pEPS1 containing a truncated *AtSUC2* promotor of only 945 bp. Both pEP1 and pEPS1 were used for the transformation of Arabidopsis (Truernit and Sauer, 1995) and

tobacco plants (Horsch et al., 1985). Ten independent transgenic Arabidopsis plants and five tobacco plants were analyzed.

Microscopic Detection of GFP Fluorescence

GFP fluorescence of whole plants, individual organs, or tissue sections was monitored under a fluorescence phase microscope (Zeiss Axioskop; Carl Zeiss, Jena, Germany) or a stereo microscope (Zeiss SV11; Carl Zeiss) after excitation with light of 460- to 500-nm wavelengths. Emitted fluorescence was photographed on Kodak Ektachrome 400 film, using a filter for the detection of fluorescence light at wavelengths longer than 510 nm. For imaging of whole Arabidopsis leaves at higher magnifications (Figures 2 and 4), images of overlapping regions from one leaf were taken and stored individually. For reconstruction of the image of a whole leaf, the individual images were montaged using the Photoshop software (Adobe, Mountain View, CA). Ovules of GFP-expressing Arabidopsis plants were viewed with an MRC 1000 confocal laser scanning microscope (Bio-Rad) using blue laser excitation light (488 nm). Scans of the resulting green (from GFP) and red (from chlorophyll) fluorescence were superimposed to reveal GFP localization inside the ovule.

Grafting of Tobacco Plants

For confirmation of GFP mobility in sieve elements, we grafted scions of wild-type tobacco plants onto rootstocks of transgenic tobacco plants expressing the *GFP* under the control of the *AtSUC2* promoter. Scions carrying two leaves between 0.5 and 1 cm were taken from the tips of wild-type plants, stuck into a vertical cut that was made in the stem of a decapitated transgenic rootstock, and fixed with tape. To avoid desiccation, grafted plants were kept under a white plastic bag for 3 to 5 days in the growth chamber. After 7 to 10 days, newly developed sink leaves of the scion ($\leqslant$1 cm) were harvested and stored in liquid nitrogen.

Extraction of the GFP from Tobacco Plants, SDS Gels, and Protein Gel Blots

Frozen sink leaves from grafted tobacco scions were homogenized in a mortar in the presence of 2 $\times$ SDS sample buffer (Laemmli, 1970). The frozen powder was thawed in the presence of 1/100 volume of a protease inhibitor mix (100 mM phenylmethylsulfonyl fluoride and 250 mM *p*-aminobenzamidine in dimethylformamide), solubilized for 5 min at 95°C, and centrifuged for 5 min at 14,000*g* to remove insoluble material. The supernatant was stored at -20°C. Equal amounts of supernatants from preparations of transgenic or wild-type tobacco plants or of wild-type tobacco plants that had been grafted onto transgenic tobacco plants were separated on SDS–polyacrylamide gels (Laemmli, 1970) and transferred to nitrocellulose filters by electroblotting (Dunn, 1986). The GFP was detected with a polyclonal anti-GFP antiserum (Clonetech, Palo Alto, CA) and an enhanced chemiluminescence Western blotting detection kit (Amersham Life Science, Braunschweig, Germany).

GUS Histochemical Staining

GUS histochemical staining of Arabidopsis plants expressing GUS under the control of the *AtSUC2* promoter (Truernit and Sauer, 1995) was performed as described previously (Truernit and Sauer, 1995) by using the substrates 4-methylumbelliferyl β-D-glucuronide (yielding a blue color; Biosynth AG, Staad, Switzerland) or 2-(2,4-hydroxy-3-methoxyphenyl)vinyl-1-methylquinolinium iodine (yielding a red color; Biosynth AG).

ACKNOWLEDGMENTS

We thank Winfried Neuhuber (Institute of Anatomy, University of Erlangen, Germany) for taking photographs using the confocal laser scanning microscope. This work was supported by the Deutsche Forschungsgemeinschaft (Grant No. SFB 473/A3). This article is dedicated to Dr. Widmar Tanner on his 60th birthday.

REFERENCES

Avery, G.S. (1933). Structure and development of the tobacco leaf. Am. J. Bot. **20,** 565–592.

Balachandran, S., Xiang, Y., Schobert, C., Thompson, G.A., and Lucas, W.J. (1997). Phloem sap proteins from *Cucurbita maxima* and *Ricinus communis* have the capacity to traffic cell to cell through plasmodesmata. Proc. Natl. Acad. Sci. USA **94,** 14150–14155.

Behnke, H.-D. (1989). Structure of the phloem. In Transport of Photoassimilates, D.A. Baker and J.A. Milburn, eds (New York: Longman Scientific and Technical), pp. 79–137.

Bokman, S.H., and Ward, W.W. (1981). Renaturation of *Aequorea* green-fluorescent protein. Biochem. Biophys. Res. Commun. **101,** 1372–1380.

Bostwick, D.E., Dannenhoffer, J.M., Skaggs, M.I., Lister, R.M., Larkins, B.A., and Thompson, G.A. (1992). Pumpkin phloem lectin genes are specifically expressed in companion cells. Plant Cell **4,** 1539–1548.

Bowman, J. (1994). Arabidopsis—An Atlas of Morphology and Development. (New York: Springer-Verlag).

Carrington, J.C., Kasschau, K.D., Mahajan, S.K., and Schaad, M.C. (1996). Cell-to-cell and long-distance transport of viruses in plants. Plant Cell **8,** 1669–1681.

Chalfie, M., Tu, Y., Euskirchen, G., Ward, W.W., and Prasher, D.C. (1994). Green fluorescent protein as a marker for gene expression. Science **263,** 802–805.

Chiu, W., Niwa, Y., Zeng, W., Hirano, T., Kobayashi, H., and Sheen, J. (1996). Engineered GFP as a vital reporter in plants. Curr. Biol. **6,** 325–330.

Clément, C., and Audran, J.C. (1995). Anther wall layers control pollen sugar nutrition in *Lilium.* Protoplasma **187,** 172–181.

Cronshaw, J. (1981). Phloem structure and function. Annu. Rev. Plant Physiol. **32,** 465–484.

Ding, B., Parthasarathy, M.V., Niklas, K., and Turgeon, R. (1988). A morphometric analysis of the phloem-unloading pathway in developing tobacco leaves. Planta **156,** 345–358.

Ding, X.S., Shintaku, M.H., Arnold, S.A., and Nelson, R.S. (1995). Accumulation of mild and severe strains of tobacco mosaic virus in minor veins of tobacco. Mol. Plant-Microbe Interact. **8,** 32–40.

Dunn, S.D. (1986). Effects of the modification of transfer buffer composition on the renaturation of proteins in gels and on the recognition of proteins on western blots by monoclonal antibodies. Anal. Biochem. **157,** 144–153.

Fellows, R.J., and Geiger, D.R. (1974). Structural and physiological changes in sugar beet leaves during sink to source conversion. Plant Physiol. **54,** 877–885.

Fisher, D.B., Wu, Y., and Ku, M.S.B. (1992). Turnover of soluble proteins in the wheat sieve tube. Plant Physiol. **100,** 1433–1441.

Fujiwara, T., Giesman-Cookmeyer, D., Ding, B., Lommel, S.A., and Lucas, W.J. (1993). Cell-to-cell trafficking of macromolecules through plasmodesmata potentiated by the red clover necrotic mosaic virus movement protein. Plant Cell **5,** 1783–1794.

Gamalei, Y.V. (1989). Structure and function of leaf minor veins in trees and herbs: A taxonomic review. Trees **3,** 96–110.

Goodwin, P.B. (1983). Molecular size limit for movement in the symplast of the *Elodea* leaf. Planta **157,** 124–130.

Hanahan, D. (1983). Studies on transformation of *E. coli* with plasmids. J. Mol. Biol. **166,** 557–580.

Ho, L.C., and Shaw, A.F. (1977). Carbon economy and translocation of ^{14}C in leaflets of the seventh leaf of tomato during leaf expansion. Ann. Bot. **41,** 833–848.

Horsch, R.B., Fry, J.E., Hoffmann, N.L., Eichholtz, D., Rogers, S.G., and Fraley, R.T. (1985). A simple and general method for transferring genes into plants. Science **227,** 1229–1231.

Ishiwatari, Y., Honda, C., Kawashima, I., Nakamura, S., Hirano, H., Mori, S., Fujiwara, T., Hayashi, H., and Chino, M. (1995). Thioredoxin h is one of the major proteins in rice phloem sap. Planta **195,** 456–463.

Ishiwatari, Y., Fujiwara, T., McFarland, K.C., Nemoto, K., Hayashi, H., Chino, M., and Lucas, W.J. (1998). Rice phloem thioredoxin h has the capacity to mediate its own cell-to-cell transport through plasmodesmata. Planta **205,** 12–22.

Jefferson, R.A., Kavanagh, T.A., and Bevan, M. (1987). GUS-fusions: β-Glucuronidase as a sensitive and versatile gene fusion marker in higher plants. EMBO J. **6,** 3901–3907.

Kempers, R. and van Bel, A.J.E. (1997). Symplasmic connections between sieve element and companion cell in the stem phloem of *Vicia faba* L. have a molecular exclusion limit of at least 10 kDa. Planta **201,** 195–201.

Kühn, C., Francheschi, V.R., Schulz, A., Lemoine, R., and Frommer, W.B. (1997). Macromolecular trafficking indicated by localization and turnover of sucrose transporters in enucleate sieve elements. Science **275,** 1298–1300.

Laemmli, U.K. (1970). Cleavage of structural proteins during the assembly of the head of bacteriophage T4. Nature **227,** 680–685.

Leisner, S.M, Turgeon, R., and Howell, S.H. (1992). Long-distance movement of cauliflower mosaic virus in infected turnip plants. Mol. Plant-Microbe Interact. **5,** 41–47.

Lucas, W.J., and Gilbertson, R.L. (1994). Plasmodesmata in relation to viral movement within leaf tissues. Annu. Rev. Phytopathol. **32,** 387–411.

Lucas, W.J., Bouché-Pillon, S., Jackson, D.P., Nguyen, L., Baker, L., Ding, B., and Hake, S. (1995). Selective trafficking of KNOTTED1 homeodomain protein and its mRNA through plasmodesmata. Science **270,** 1980–1983.

Maule, A.J. (1991). Virus movement in infected plants. Crit. Rev. Plant Sci. **9,** 457–473.

Murillo, I., Cavallarin, L., and San Segundo, B. (1997). The maize pathogenesis-related PRms protein localizes to plasmodesmata in maize radicles. Plant Cell **9,** 145–156.

Nakamura, S., Hayashi, H., Mori, S., and Chino, M. (1993). Protein phosphorylation in the sieve tubes of rice plants. Plant Cell Physiol. **34,** 927–933.

Nelson, R.S., and van Bel, A.J.E. (1998). The mystery of virus trafficking into, through and out of vascular tissue. Prog. Bot. **59,** 476–533.

Ooms, G., Hoykaas, P.J.J., Van Veen, R.J.M., Van Beelen, P., Regensburg-Tuink, T.J.G., and Schilperoort, R.B. (1982). Octopine Ti-plasmid deletion mutants of *Agrobacterium tumefaciens* with emphasis on the right side of the T-region. Plasmid **7,** 15–29.

Oparka, K.J., Duckett, C.M., Prior, D.A.M., and Fisher, D.B. (1994). Real-time imaging of phloem unloading in the root tip of *Arabidopsis.* Plant J. **6,** 759–766.

Ormö, M., Cubitt, A.B., Kallio, K., Gross, L.A., Tsien, R.Y., and Remington, S.J. (1996). Crystal structure of the *Aequorea victoria* green fluorescent protein. Science **273,** 1392–1395.

Pacini, E., and Franchi, G.G. (1983). Pollen grain development in *Smilax aspersa* L. and possible functions of the loculus. In Pollen: Biology and Implications for Plant Breeding, D.L. Mulcahy and E. Ottavino, eds (New York: Elsevier), pp. 183–190.

Raven, J.A. (1991). Long-term functioning of enucleate sieve elements: Possible mechanisms of damage avoidance and damage repair. Plant Cell Environ. **14,** 139–146.

Roberts, A.G., Santa Cruz, S., Roberts, I.M., Prior, D.A.M., Turgeon, R., and Oparka, K.J. (1997). Phloem unloading in sink leaves of *Nicotiana benthamiana*: Comparison of a fluorescent solute with a fluorescent virus. Plant Cell **9,** 1381–1396.

Sakuth, T., Schobert, C., Pecsvaradi, A., Eichholz, A., Komor, E., and Orlich, G. (1993). Specific proteins in the sieve-tube exudate of *Ricinus communis* L. seedlings: Separation, characterization and in-vivo labeling. Planta **191,** 207–213.

Sanger, F., Nicklen, S., and Coulson, A.R. (1977). DNA sequencing with chain terminating inhibitors. Proc. Natl. Acad. Sci. USA **74,** 5463–5467.

Schobert, C., Grossmann, P., Gottschalk, M., Komor, E., Pecsvaradi, A., and zur Nieden, U. (1995). Sieve-tube exudate from *Ricinus communis* L. seedlings contains ubiquitin and chaperons. Planta **196,** 205–210.

Sjölund, R.D. (1997). The phloem sieve element: A river runs through it. Plant Cell **9,** 1137–1146.

Stadler, R., and Sauer, N. (1996). The *Arabidopsis thaliana AtSUC2* gene is specifically expressed in companion cells. Bot. Acta **109,** 299–306.

Truernit, E., and Sauer, N. (1995). The promoter of the *Arabidopsis thaliana SUC2* sucrose-H^+ symporter gene directs expression of β-glucuronidase to the phloem: Evidence for phloem loading and unloading by SUC2. Planta **196,** 564–570.

Truernit, E., Stadler, R., Baier, K., and Sauer, N. (1999). A male gametophyte–specific monosaccharide transporter in *Arabidopsis.* Plant J. **17,** 191–201.

Tucker, E.B. (1982). Translocation in the staminal hairs of *Setcreasea purpurea.* I. A study of cell ultrastructure and cell-to-cell passage of molecular probes. Protoplasma **113,** 193–201.

Turgeon, R. (1989). The sink–source transition in leaves. Annu. Rev. Plant Mol. Biol. **40,** 119–138.

Turgeon, R., and Webb, J.A. (1973). Leaf development and phloem transport in *Cucurbita pepo*: Transition from import to export. Planta **113,** 179–191.

Wang, N., and Fisher, D.B. (1994a). Monitoring phloem unloading and post-phloem transport by microperfusion of attached wheat grains. Plant Physiol. **104,** 7–16.

Wang, N., and Fisher, D.B. (1994b). The use of fluorescent tracers to characterize the post-phloem transport pathway in maternal tissues of developing wheat grains. Plant Physiol. **104,** 17–27.

Ward, W.W. (1981). Properties of the coelenterate green-fluorescent protein. In Bioluminescence and Chemiluminescence: Basic Chemistry and Analytical Applications, M. DeLuca and W.D. McElroy, eds (New York: Academic Press), pp. 235–242.

Weber, H., Borisjuk, L., Heim, U., Sauer, N., and Wobus, U. (1997). A role for sugar transporters during seed development: Molecular characterization of a hexose and a sucrose carrier in fava bean seeds. Plant Cell **9,** 895–908.

Wolf, S., Deom, C.M., Beachy, R.N., and Lucas, W.J. (1989). Movement protein of tobacco mosaic virus modifies plasmodesmata size exclusion limit. Science **246,** 377–379.